Received: 20 September 2016 | Revised: 24 November 2016 | Accepted: 3 December 2016

DOI 10.1002/aoc.3724

WILEY Applied Organometallic Chemistry

FULL PAPER

Synthesis, characterization, and biological and anticancer studies of mixed ligand complexes with Schiff base and 2,2′-bipyridine

M.M. Omar[1] | Hanan F. Abd El-Halim[2] | Eman A.M. Khalil[3]

[1] Chemistry Department, Faculty of Science, Cairo University, 12613 Giza, Egypt

[2] Pharmaceutical Chemistry Department, Faculty of Pharmacy, Misr International University, Cairo, Egypt

[3] Faculty of Physical Therapy, Modern University for Technology and Information, Cairo, Egypt

Correspondence
Hanan F. Abd El-Halim, Pharmaceutical Chemistry Department, Faculty of Pharmacy, Misr International University, Cairo, Egypt.
Email: hanan.farouk2@yahoo.com; hanan_farouk1@hotmail.com

New mixed ligand complexes of transition metals were synthesized from a Schiff base (L^1) obtained by the condensation reaction of oxamide and furfural as primary ligand and 2,2′-bipyridine (L^2) as secondary ligand. The ligands and their metal complexes were studied using various spectroscopic methods. Also thermal analyses were conducted. The mixed ligand complexes were found to have formulae $[M(L^1)(L^2)]Cl_m{\cdot}nH_2O$ (M = Cr(III) and Fe(III): $m = 3$, $n = 0$; M = Cu(II) and Cd(II): $m = 2$, $n = 1$; M = Mn(II), Co(II), Ni(II) and Zn(II): $m = 2$, $n = 0$). The resultant data revealed that the metal complexes have octahedral structure. Also, the mixed ligand complexes are electrolytic. The biological and anticancer activities of the new compounds were tested against breast cancer (MCF-7) and colon cancer (HCT-116) cell lines. The results showed high activity for the synthesized compounds.

KEYWORDS

2,2′-bipyridine, anticancer activity, biological activity, mixed ligand complexes, Schiff base ligand

1 | INTRODUCTION

Study of coordination chemistry of transition metal ions with various types of ligands has been enhanced by the current advancements in the fields of bioinorganic chemistry and medicine.[1] Through the years, Schiff bases have played a special role as chelating ligands in main group and transition metal coordination chemistry, due to their stability under a variety of oxidative and reductive conditions, and to the fact that imine ligands are borderline between hard and soft Lewis bases.[2–4] Schiff bases that arise from amino and carbonyl compounds are an important class of ligands that coordinate to metal ions through azomethine nitrogen and have been studied widely.[5] In azomethine derivatives, the (C═N) linkage is necessary for biological activity; numerous azomethines have been reported to have marked antifungal, antibacterial, anticancer and antimalarial activities.[6–14] A large number of Schiff bases and their complexes have been studied for their interesting and significant properties, e.g. their ability to reversibly bind oxygen,[15,16] catalytic activity in hydrogenation of olefins,[17] photochromic properties[18] and complexing ability towards some toxic metals.[19]

Mixed ligand complexes also play an important role in the biological field as exemplified by many ways in which enzymes are known to be activated by metal ions.[20] Schiff bases derived from heterocyclic compounds such as furan-2-carbaldehyde have attracted an increased interest in the bioinorganic chemistry field.[21–23] Furfural is an important renewable, non-petroleum-based and chemical raw material. It is used to make other furan chemicals, such as furoic acid, via oxidation[24] and also is considered as an important chemical solvent.

Oxamide derivatives have a wide range of applications in bioinorganic chemistry, for example in medical applications, as markers for analytical targets, and small molecular gelators of organic liquids.[25,26] Many oxamide derivatives also exhibit biological activity, such as plant growth regulators, pesticides or HIV-1 protease inhibitors.[25]

Since the discovery of bipyridine at the end of the nineteenth century, the bipyridine ligand has been used extensively in the complexation of metal ions due to its strong redox stability and ease of functionalization.[27,28]

In the study reported here, the coordination behaviour of a Schiff base derived from the condensation of oxamide with

 Copyright © 2017 John Wiley & Sons, Ltd.

2-furancarboxaldehyde (L^1) as a primary ligand in the presence of 2,2′-bipyridine (L^2) as a secondary ligand towards some transition metal ions, namely Cr(III), Mn(II), Fe(III), Co(II), Ni(II), Cu(II), Zn(II) and Cd(II), has been studied. Characterization of the Schiff base ligand and the mixed ligand complexes was conducted using elemental analyses, infrared (IR), mass, ^{1}H NMR, UV–visible, solid reflectance and electron spin resonance (ESR) spectroscopies, molar conductance, magnetic susceptibility, X-ray diffraction (XRD) and thermal analyses (thermogravimetry (TG) and differential thermogravimetry (DTG)). The biological and anti-tumour activities of the Schiff base and its mixed ligand complexes were investigated.

2 | EXPERIMENTAL

2.1 | Materials

All reagents were acquired commercially of analytical grade (AR) and of highest purity available. They included furan-2-carboxaldehyde (Sigma), oxamide (Acros) and 2,2′-bipyridine (Fluka Chemie AG). $CrCl_3{\cdot}6H_2O$, $CuCl_2{\cdot}2H_2O$ and $MnCl_2{\cdot}2H_2O$ (Sigma), $FeCl_3{\cdot}6H_2O$ (Prolabo), $CoCl_2{\cdot}6H_2O$, $NiCl_2{\cdot}6.H_2O$ and $ZnCl_2{\cdot}2H_2O$ (BDH) and $CdCl_2{\cdot}2H_2O$ (Aldrich) were used. Organic solvents were spectroscopically pure from BDH and included absolute ethanol and dimethylformamide (DMF). Deionized water collected from all-glass equipment was usually utilized in all preparations.

2.2 | Solutions

A fresh stock solution (1×10^{-3} M) of L^1 ligand was prepared in 5 ml of DMF. Stock solutions (1×10^{-3} M) of the metal complexes (Cr(III), 0.636; Mn(II), 0.526; Fe(III), 0.562; Co(II), 0.584; Ni(II), 0.584; Cu(II), 0.552; Zn(II), 0.572; and Cd(II), 0.636 g l^{-1} were prepared by dissolving accurately weighed amounts in 5 ml of DMF. The metal complexes solutions were standardized using recommended procedures.[29]

2.3 | Instrumentation

At the Microanalytical Center, Cairo University, Egypt, elemental analyses were carried out using a CHNS-932 (LECO) Vario elemental analyser. The molar conductance measurements were carried out utilizing a Sybron-Barnstead conductometer. Mass spectra were recorded using the electron impact technique at 70 eV using an MS-5988 GS–MS Hewlett-Packard instrument at the National Center for Research, Egypt. Molar magnetic susceptibilities were measured with powdered samples utilizing the Faraday method. IR spectra were recorded with a PerkinElmer FT-IR type 1650 spectrophotometer in the wavenumber region 400–4000 cm^{-1}. The spectra were recorded as KBr pellets. ^{1}H NMR spectra, as solutions in deuterated dimethylsulfoxide (DMSO-d_6), were recorded with a 300 MHz Varian-Oxford Mercury at room temperature utilizing tetramethylsilane (TMS) as an internal standard. Solid reflectance spectra were measured with a Shimadzu 3101pc spectrophotometer. ESR spectra were recorded utilizing a Bruker EMX EPR spectrometer located in the National Center for Radiation Research and Technology at the Atomic Energy Authority. Powder XRD analyses were carried out also at the Atomic Energy Authority. TG and DTG analyses were carried out in dynamic nitrogen atmosphere (20 ml min^{-1}) with a heating rate of 10 °C min^{-1} using a Shimadzu TGA-50H thermal analyser. Spectrophotometric measurements in solution were carried out utilizing an automated UV–visible spectrophotometer (PerkinElmer Lambda 20) from 200 to 700 nm. The antibacterial, antifungal and anticancer activities were determined at the Regional Center for Fungi and their Applications, Al-Azhar University, Egypt.

2.4 | Procedures

2.4.1 | Preparation of Schiff base ligand

A hot ethanolic (5 ml) solution of 22.72 mmol of aldehyde (furan-2-carbaldehyde) was condensed with oxamide (11.36 mmol, 1 g) dissolved in a hot (70 °C) DMF–ethanol mixture (3:1 *v*/v) in 2:1 molar ratio. The reaction mixture was left under reflux for 3–4 h. A pale brown precipitate was obtained, filtered, washed with ethanol and dried under vacuum over calcium chloride. The structure of the Schiff base ligand is shown in Figure 1.

2.4.2 | Preparation of mixed ligand complexes

The appropriate quantity of Schiff base ligand (2 mmol, 0.5 g) dissolved in absolute DMF (20 ml) as a primary ligand was mixed with 2,2′-bipyridine (2 mmol, 0.31 g) dissolved in absolute ethanol as a secondary ligand, and then a hot ethanolic solution of metal chloride salt (2 mmol, 0.53 g of $CrCl_3{\cdot}6H_2O$, 0.32 g of $MnCl_2{\cdot}2H_2O$, 0.54 g of $FeCl_3{\cdot}6H_2O$, 0.47 g of $CoCl_2{\cdot}6H_2O$, 0.47 g of $NiCl_2{\cdot}6H_2O$, 0.34 g of $CuCl_2{\cdot}2H_2O$, 0.34 of $ZnCl_2{\cdot}2H_2O$ and 0.43 g of $CdCl_2{\cdot}2H_2O$) was added dropwise to the mixed ligands. The mixture was refluxed for 1–2 h with stirring. The precipitates were filtered, washed several times with cold ethanol and dried under vacuum over anhydrous $CaCl_2$. The suggested structures of the mixed ligand complexes are presented in Figure 2. The reaction is as follows:

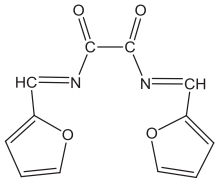

FIGURE 1 Structure of Schiff base ligand (L^1)

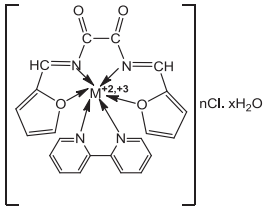

FIGURE 2 General structure of mixed ligand complexes. M(II) = Mn, Co, Ni, Cu, Zn, Cd; $n = 2$; $x = 0, 1$. M(III) = Cr, Fe; $n = 3$; $x = 0$

$$L^1 + L^2 + M(II) \text{ or } M(III) \rightarrow \left[M\left(L^1\right)\left(L^2\right)\right]Cl_n \cdot xH_2O$$

where M(II) = Mn, Co, Ni, Cu, Zn, Cd; M(III) = Cr, Fe; $n = 2, 3$; $x = 0, 1$.

2.4.3 | Antimicrobial activity

The antimicrobial activity of samples was determined using the agar well diffusion method.[30] Sterilized medium was poured onto sterilized Petri dishes (20 ml each) and allowed to solidify. Wells of 6 mm in diameter were made in the hardened medium using a sterile borer. A sterile swab was used to evenly distribute microbial suspension over the surface of hardened medium and solutions of the tested samples were added to each well using a micropipette. The plates were incubated at 37 °C for 24 h in case of antibacterial activity and 48 h at 25 °C for antifungal activity. This experiment was conducted in triplicate and zones of inhibition were measured in millimetres.

2.4.4 | Anti-tumour activity

Cells were propagated in Dulbecco's modified Eagle's medium supplemented with 10% heat-inactivated foetal bovine serum, 1% L-glutamine, HEPES buffer and 50 μg ml^{-1} gentamycin. All cells were maintained at 37 °C in a humidified atmosphere with 5% CO_2 and were sub-cultured two times a week.

For cytotoxicity assay, the cells were seeded in a 96-well plate at a cell concentration of 1×10^4 cells per well in 100 μl of growth medium. Fresh medium containing various concentrations of test sample was added after 24 h of seeding. Serial two-fold dilutions of the tested chemical compound were added to confluent cell monolayers dispensed into 96-well, flat-bottomed microtitre plates (Falcon, NJ, USA) using a multichannel pipette. The microtitre plates were incubated at 37 °C in a humidified incubator with 5% CO_2 for a period of 48 h. Three wells were used for each concentration of test sample. Control cells were incubated without test sample and with or without DMSO. The small percentage of DMSO present in the wells (maximal 0.1%) was found not to affect the experiment. After incubation of the cells for 24 h at 37 °C, various concentrations of sample (50, 25, 12.5, 6.25, 3.125 and 1.56 μg) were added, and incubation was continued for 48 h and viable cell yield was determined using a colorimetric method.

In brief, after the end of the incubation period, media were aspirated and crystal violet solution (1%) was added to each well for at least 30 min. The stain was removed and the plates were rinsed with tap water until all excess stain was removed. Glacial acetic acid (30%) was then added to all wells and mixed thoroughly, and then the absorbance of the plates was measured after gently shaken on a microplate reader (Tecan Inc.), using a test wavelength of 490 nm. All results were corrected for background absorbance measured in wells without added stain. Treated samples were compared with the cell control in the absence of the tested compounds. All experiments were carried out in triplicate. The cell cytotoxic effect of each tested compound was calculated.[31]

3 | RESULTS AND DISCUSSION

3.1 | Elemental analyses and molar conductivity measurements

The results of elemental analysis for the Schiff base ligand and its mixed ligand complexes are in good agreement with the calculated values. The mixed ligand complexes were dissolved in DMF and the molar conductivities of their solutions (10^{-3} M) at 25 ± 2 °C were measured. It is concluded from the results that Mn(II), Co(II), Ni(II), Cu(II), Zn(II) and Cd(II) complexes are ionic in nature and are of type 2:1 electrolytes. It is also concluded from the results that the Cr(III) and Fe(III) mixed ligand complexes, having molar conductance values of 230 and 324 Ω^{-1} mol^{-1} cm^2, respectively, are ionic in nature and considered as 3:1 electrolytes. These results also indicate the non-bonding of the chloride anions to the metal ions. The results are listed in Table 1.

3.2 | IR spectra

The IR spectra of the mixed ligand complexes were compared with that of the free Schiff base ligand L^1 to determine the coordination sites that might be involved in chelation. The data are summarized in Table 2. The small and sharp bands observed at 1607 and 1661 cm^{-1} in the spectrum of free Schiff base ligand are assigned to the ν(C═N) and ν(C═O) stretching vibrations, respectively. In the metal complex spectra, the ν(C═N) stretching vibration of the azomethine is shifted to higher or lower wavenumbers which might indicate the participation of the azomethine nitrogen in coordination.[32,33]

The ν(C═O) stretching vibrations are observed at 1655–1678 cm^{-1} for the mixed ligand complexes. The latter region corresponds the uncoordinated amide (C═O) group.[34] The band at 650 cm^{-1} is assigned to ν(C═N) of pyridine for secondary ligand L^2. This band is shifted to 671–682 cm^{-1} for mixed ligand complexes.[33,35] The furan oxygen stretching band assigned at 1226 cm^{-1} for free Schiff base ligand is shifted to higher wavenumbers in the spectra of mixed ligand complexes by 20–35 cm^{-1}. This indicates the participation of the furan oxygen atom in coordination.[36] New bands of low

TABLE 1 Analytical and physical data for L^1 and its mixed ligand complexes

Compound (chemical formula)	Colour	Yield (%)	M.p. (°C)	Found (calcd) C (%)	H (%)	N (%)	M (%)	μ_{eff} (BM)	Λ_m (Ω^{-1} mol^{-1} cm^2)
L^1	Pale brown	72.2	210	59.43 (59.01)	3.11 (3.27)	10.98 (11.47)	—	—	—
$[Cr(L^1)(L^2)]Cl_3$	Pale brown	70	280	47.46 (47.26)	3.01 (2.86)	9.88 (10.02)	8.29 (9.33)	3.52	230
$[Mn((L^1)(L^2)]Cl_2$	Beige	65	270	50.54 (50.19)	3.12 (3.04)	10.24 (10.66)	10.43 (10.46)	5.33	140
$[Fe(L^1)(L^2)]Cl_3$	Reddish brown	71	270	46.35 (46.93)	2.96 (2.84)	10.21 (9.95)	11.70 (12.08)	1.85	324
$[Co(L^1)(L^2)]Cl_2$	Brown	69	280	49.23 (49.81)	3.44 (3.01)	10.18 (10.56)	9.45 (11.13)	4.86	134
$[Ni(L^1)(L^2)]Cl_2$	Pale beige	76	>300	50.12 (49.81)	3.55 (3.01)	10.98 (10.56)	10.20 (11.13)	2.24	129
$[Cu(L^1)(L^2)]Cl_2{\cdot}H_2O$	Green olive	75	290	47.82 (47.78)	3.78 (3.25)	9.83 (10.13)	11.00 (11.60)	1.98	265
$[Zn(L^1)(L^2)]Cl_2$	Pale beige	87	280	49.56 (49.25)	3.01 (2.98)	10.21 (10.44)	11.12 (12.14)	—	160
$[Cd(L^1)(L^2)]Cl_2{\cdot}H_2O$	Silver	80	>300	43.56 (43.92)	3.21 (2.99)	9.67 (9.31)	16.13 (15.82)	—	168

TABLE 2 IR bands (400–4000 cm^{-1}) of L^1, L^2 and transition metal mixed ligand complexes[a]

Compound	ν(C=N)	ν(C=O)	ν(C—O)	ν(C—N)	ρ(Py) bending	ν(M—O)	ν(M—N)
L^1	1607 s	1661 sh	1226w	1095 sh	—	—	—
L^2	1642 m	—	—	1135 s	650 s	—	—
$[Cr(L^1)(L^2)]Cl_3$	1612 w	1678 w	1253w	1102 sh	678 m	471 sh	401 s
$[Mn((L^1)(L^2)]Cl_2$	1608 s	1670 m	1261w	1103 m	675 m	469 sh	420 s
$[Fe(L^1)(L^2)]Cl_3$	1614 s	1670 m	1257w	1103 sh	671 m	470 sh	412 w
$[Co(L^1)(L^2)]Cl_2$	1612 s	1666 s	1257w	1104 sh	675 m	473 sh	417 s
$[Ni(L^1)(L^2)]Cl_2$	1613 s	1671 m	1253w	1103 sh	671 s	470 sh	428 s
$[Cu(L^1)(L^2)]Cl_2{\cdot}H_2O$	1601 m	1655 m	1248s	1103 sh	671 s	471 m	420 m
$[Zn(L^1)(L^2)]Cl_2$	1615 s	1678 w	1250w	1101 sh	682 s	478 sh	428 w
$[Cd(L^1)(L^2)]Cl_2{\cdot}H_2O$	1593 m	1659 m	1246s	1107 m	672 m	471 m	413 m

[a]sh, sharp; m, medium; s, small; w, weak; br, broad.

intensity in the spectra of all complexes are observed at 401–428 and 469–478 cm^{-1}. These bands are assigned to ν(M—N) and ν(M—O) stretching vibrations, respectively.

3.3 | Mass spectrum of schiff base ligand

Mass spectrometry plays an important role in elucidating the molar weight and structure of ligands and complexes. The electron impact mass spectrum of the new Schiff base ligand was recorded and the important peaks and their relative intensities for the molecular ions are shown in Scheme 1. The mass spectrum of the studied Schiff base is characterized by moderate to high relative intensity molecular ion peaks at 70 eV. The mass spectrum of the Schiff base ligand shows a well-defined parent peak of L^1 at m/z = 244 (RI = 1%) which is in agreement with the formula $C_{12}H_8N_2O_4$ and is equivalent to its molecular weight. The other molecular ion peaks appearing in the mass spectrum may be attributed to the fragmentation of the Schiff base ligand as a result of the rupture of different bonds inside the molecule.

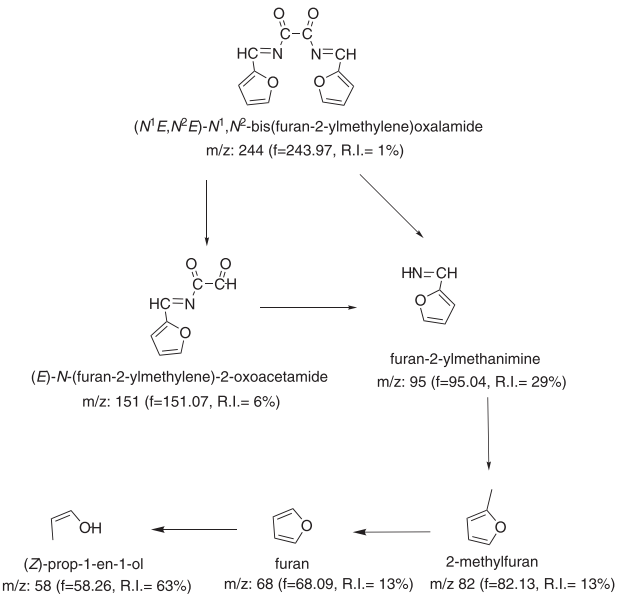

SCHEME 1 Mass fragmentation pattern of Schiff base ligand L^1

3.4 | ^{1}H NMR spectra

The Schiff base ligand and its Zn(II) and Cd(II) mixed ligand chelates were characterized by ^{1}H NMR spectra to elucidate the differently positioned protons. The ^{1}H NMR spectra of L^1 Schiff base and its Zn(II) and Cd(II) mixed ligand complexes were recorded in DMSO-d_6 solution using TMS as an internal standard. The ^{1}H NMR spectrum of the Schiff base ligand shows a signal at 7.95 ppm which is attributed

to the azomethine (—C═N—) protons. The ligand also reveals another singlet signal at 7.66 ppm which is attributed to furan ring protons. On chelation, the position of azomethine signal is shifted to higher value, 8.71 and 8.67 ppm for Zn(II) and Cd(II) complexes, respectively. In comparison with that of the free ligand value, this is assigned to coordination through the azomethine nitrogen atom of the Schiff base ligand.[37] Multiplets assigned to the pyridine and furan ring protons are displaced downfield around the region 7.67–8.09 ppm, which indicates the possibility of the involvement of oxygen of furan ring in the coordination.

3.5 | UV–visible spectra

The electronic spectral data were recorded for the free Schiff base ligand and its mixed ligand complexes in DMF solvent in the range 200–700 nm at room temperature using the same solvent as blank. The Schiff base ligand shows two bands at 254 and 281 nm. The first band at 254 nm might be attributed to π–π* transition of the heterocyclic moieties.[38] The second band appearing at 281 nm might be attributed to the n–π* transition of the azomethine group. The d–d transitions could not be seen because of their weakness.[20,39] Due to the coordination of azomethine nitrogen of the Schiff base ligand to the metal ions in the mixed ligand chelates, the n–π* transition band is observed in the absorption spectra of all mixed ligand complexes at 277–301 nm.[40]

3.6 | Magnetic susceptibility

The magnetic moment values are presented in Table 1. The magnetic moment values for Cr(III), Mn(II), Fe(II), Co(II), Ni(II) and Cu(II) complexes are found to be 3.52, 5.33, 1.85, 4.86, 2.24 and 1.98 BM, respectively, which suggest an octahedral geometry.[35,41,42] The Zn(II) and Cd(II) complexes are diamagnetic.

3.7 | Diffuse reflectance spectral studies

The electronic spectrum of Cr(III) complex exhibits three bands at 22 222, 19 417 and 16 821 cm^{-1} that can be assigned to $^4A_{2g}(F) \rightarrow {}^4T_{1g}(P)$, $^4A_{2g}(F) \rightarrow {}^4T_{2g}(F)$ and $^4A_{2g}(F) \rightarrow {}^4T_{2g}(F)$ transitions, respectively, suggesting an octahedral geometry for Cr(III) complex.[42,43] The electronic spectrum of Mn(II) complex shows three bands at 25 381, 19 157 and 16 474 cm^{-1}, which may be assigned to $^4T_{1g} \rightarrow {}^6A_{1g}$, $^4T_{2g}(G) \rightarrow {}^6A_{1g}$ and $^4T_{1g}(D) \rightarrow {}^6A_{1g}$, transitions, respectively, which suggest an octahedral geometry.[35,42]

From the diffuse reflectance spectrum, it is observed that the Fe(III) chelate exhibits a band at 21 276 cm^{-1} which may be assigned to the $^6A_{1g} \rightarrow T_{2g}(G)$ transition in octahedral geometry of the complex.[42–44] The $^6A_{1g} \rightarrow {}^5T_{1g}$ transition is split into two bands at 16 000 and 13 262 cm^{-1}, respectively, which indicates an octahedral geometry for Fe(III) complex involving d^2sp^3 hybridization in Fe(III) ion.[42] The diffuse reflectance spectrum of Co(II) complex shows three bands at 21 345, 16 892 and 13 680 cm^{-1}. The band at 25 974 cm^{-1} corresponds to ligand-to-metal charge transfer band. The bands observed are assigned to the $^4T_{1g}(F) \rightarrow {}^4T_{2g}(P)$, $^4T_{1g}(F) \rightarrow {}^4A_{2g}(F)$ and $^4T_{1g}(F) \rightarrow {}^4T_{2g}(F)$ transitions, respectively, indicating that there is an octahedral geometry around Co(II) ion.[42–45]

The solid reflectance spectrum of Ni(II) complex shows three bands at 22 173, 16 920 and 12 878 cm^{-1} which may be assigned to $^3A_{2g} \rightarrow {}^3T_{1g}(P)$, $^3A_{2g} \rightarrow {}^3T_{1g}(F)$ and $^3A_{2g} \rightarrow {}^3T_{2g}$ transitions, respectively, suggesting that the Ni(II) complex has an octahedral geometry.[46] The spectrum shows also a band at 25 252 cm^{-1} which may be attributed to ligand-to-metal charge transfer. The electronic spectrum of Cu(II) complex shows a band at 17 331 cm^{-1}, which indicates the presence of a transition from d_{xy}, d_{z2} and d_{xz}, d_{yz} transfer to the antibonding and half-filled $d_{x^2-y^2}$ level which is indicative of an octahedral configuration, and a band at 40 322 cm^{-1} which may correspond to ligand-to-metal charge transfer.[47–51] The Zn(II) and Cd(II) complexes are diamagnetic.

3.8 | ESR spectrum

The ESR spectrum of the Cu(II) complex (Figure 3) exhibits axially symmetric g-tensor parameters with $g_e < g_\perp > 2.0023$ suggesting that the copper site has a $d_{x^2-y^2}$ ground state characteristic of tetrahedral, square planer or octahedral stereochemistry.[52] The observed order for Cu(II) complex of $g_{\|}$ (2.064) > $g_\perp$ (2.02) > g_e (2.0023) indicates that the complex has an octahedral geometry.[53] Kivelson and Neiman[54] reported the $g_{\|}$ value less than 2.3 for covalent character of the metal–ligand bond and greater than 2.3 for ionic character. The $g_{\|}$ value for the Cu(II) complex is 2.0145, and consequently the environment is covalent. In axial symmetry the g-values are related by the Hathaway expression $G = (g_{\|} - 2)/(g_\perp - 2) = 4$, where G is the exchange interaction parameter. When $G < 4.0$, a considerable exchange interaction between Cu(II) centres in the solid state is disregarded ($G = 3.21$).[55]

3.9 | Powder XRD

The powder XRD patterns of all the compounds were investigated in the range 3–80° (θ) at a wavelength of 1.54 Å. The diffractogram and related data depict the 2θ value

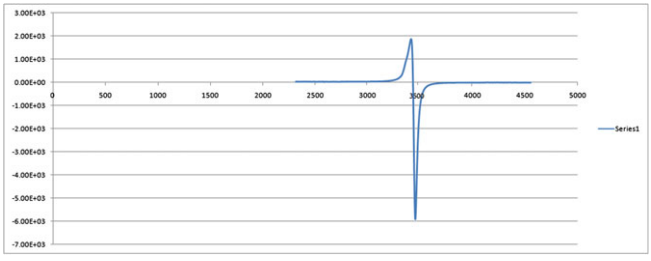

FIGURE 3 ESR spectrum of Cu(II) complex

foreach peak, relative intensity and inter-planar spacing (*d*-values). The XRD pattern of a pure substance is like a fingerprint of the substance. The XRD patterns of the complexes show that the coordination of the Schiff base ligand in the presence of 2,2′-bipyridine is of crystalline nature for Cr(III), Mn(II), Fe(III), Co(II), Ni(II), Cu(II), Zn(II) and Cd(II) complexes.

The average crystallite size (ξ) can be calculated from the XRD data according to the Debye–Scherrer equation:[56,57]

$$\xi = \frac{K\lambda}{\beta_{1/2}\cos\theta} \quad (1)$$

where the reference peak width is at the angle θ, λ is the wavelength of X-ray radiation (1.542475 Å), K is a constant taken as 0.95 for organic compounds[56] and $\beta_{1/2}$ is the width at half maximum of the reference diffraction peak measured in radians. The dislocation density (δ) is the number of dislocation lines per unit area of the crystal. The value of δ is related to the average particle diameter (ξ) by the relation[58,59]

$$\delta = \frac{1}{\xi^2} \quad (2)$$

The value of ξ was calculated and found to be in the range 23.91–46.17 nm δ for the free Schiff base ligand and its Cr(III), Mn(II), Fe(III), Co(II), Ni(II), Cu(II), Zn(II) and Cd(II) complexes. The dislocation density (δ) was also calculated and found to be in the range 0.00046–0.0017nm^{-2}.

3.10 | Thermal analysis of metal complexes

The thermal stabilities of the Schiff base ligand and its mixed ligand complexes were investigated. The results are summarized in Table 3. The TG curve of Schiff base (L^1) shows four steps of mass losses at temperature ranging from 45 to 770 °C. The decomposition of the first two steps within the range 45–430 °C corresponds to the loss of $C_2H_2O_2$ with a mass loss of 22.46% (calcd 23.70%). The decomposition of third step within the range 430–540 °C is assigned to loss of CHN with a mass loss of 10.28% (calcd 11.47%). The fourth step (540–770 °C) corresponds to the removal of remaining part of the ligand with a mass loss of 65.89% (calcd 65.16%). The overall mass loss amounts to 98.82% (calcd 100%).

The thermogram of the Cr(III) complex shows three decomposition steps within the range 45–670 °C. The first decomposition step is accompanied by loss of $^3/_2$ Cl_2 molecules in the range 45–370 °C with an estimated mass loss of 20.67% (calcd 19.06%). The second stage of decomposition corresponds to loss of C_4H_{10} molecule at 370–570 °C with an estimated mass loss of 10.05% (calcd 10.38%). The third decomposition step within the range 570–670 °C is assigned to loss of $C_{18}H_6O_3N_4$ molecule with a mass loss of 58.26% (calcd 58.37%). Thereafter the percentage of the residue corresponds to chromium oxide is 11.15% (calcd 12.19%).

The Mn(II) complex gives a decomposition pattern starting at 45 °C and finishing at 580 °C with two stages. The first stage is one step within the range 45–405 °C, attributed to the loss of HCl gas with a mass loss of 5.65% (calcd 6.93%). The second stage is also one step representing the loss of HCl gas and $C_{22}H_{14}O_3N_4$ molecule with a mass loss

TABLE 3 Thermoanalytical results of Schiff base (L^1) and its mixed ligand complexes

Compound	TG range (°C)	DTG (°C)	Number of steps	Found (calcd)		Assignment	Metallic residue
				Mass loss (%)	Total mass loss (%)		
L^1	45–430	130, 328	2	22.46 (23.70)	(98.82) (100)	Loss of $C_2H_2O_2$	–
	430–540	479	1	10.28 (11.47)		Loss of CHN	
	540–770	684	1	65.89 (65.16)		Loss of $C_9H_5O_2N$	
$[Cr(L^1)(L^2)]Cl_3$	45–370	292	1	20.67 (19.06)	88.85 (87.81)	Loss of 3/2 Cl_2	½Cr_2O_3
	370–570	495	1	10.05 (10.38)		Loss of C_4H_{10}	
	570–670	613	1	58.26 (58.37)		Loss of $C_{18}H_6O_3N_4$	
$[Mn((L^1)(L^2)]Cl_2$	45–405	359	1	5.65 (6.93)	86.53 (86.49)	Loss of HCl	MnO
	405–580	517	1	80.87 (79.56)		Loss of HCl and $C_{22}H_{14}O_3N_4$	
$[Fe(L^1)(L^2)]Cl_3$	45–350	281	1	82.62 (82.22)	82.62 (82.23)	Loss Cl_2, HCl and $C_{21}H_{15}O_2N_4$	½Fe_2O_3 + C
$[Co(L^1)(L^2)]Cl_2$	45–345	289	1	87.37 (85.85)	87.54 (85.85)	Loss of Cl_2 and $C_{22}H_{16}O_3N_4$	CoO
$[Ni(L^1)(L^2)]Cl_2$	45–360	299	1	86.78 (85.85)	86.79 (85.85)	Loss of Cl_2 and $C_{22}H_{16}O_3N_4$	NiO
$[Cu(L^1)(L^2)]Cl_2{\cdot}H_2O$	45–205	105	1	2.16 (3.20)	86.11 (85.50)	Loss of H_2O	CuO
	205–415	356	1	11.25 (12.80)		Loss of Cl_2	
	415–995	518, 623, 787	3	72.48 (69.50)		Loss of $C_{22}H_{16}O_3N_4$	
$[Zn(L^1)(L^2)]Cl_2$	45–305	260	1	36.92 (36.56)	85.90 (84.87)	Loss of Cl_2 and $C_5H_5O_2N_2$	ZnO
	305–450	402	1	23.39 (22.76)		Loss of $C_6H_6ON_2$	
	450–995	484, 598	2	25.51 (25.55)		Loss of $C_{11}H_5$	
$[Cd(L^1)(L^2)]Cl_2{\cdot}H_2O$	45–225	151	1	8.37 (9.34)	81.21 (81.06)	Loss of H_2O and HCl	CdO
	225–425	383	1	22.15 (22.02)		Loss of HCl and $C_5H_4N_2$	
	425–995	466, 530	2	50.83 (49.70)		Loss of $C_{17}H_{10}O_3N_2$	

of 80.87% (calcd 79.56%) within the range 405–580 °C. MnO is the residue with mass percent of 13.47% (calcd 13.51%).

The TG curves of Fe(III), Co(II) and Ni(II) complexes show one stage of decomposition within the range 45–350 °C. For the Fe(III) complex, this stage corresponds to the loss of HCl gas, Cl_2 gas and $C_{21}H_{15}O_2N_4$ molecule leaving ½Fe_2O_3 as a residue contaminated with carbon with mass loss of 17.38% (calcd 17.77%). However, for the other two complexes it corresponds to the loss of Cl_2 gas and $C_{22}H_{16}O_3N_4$ leaving the metal oxide as residue.

The Cu(II) complex exhibits five decomposition steps within the range 45–995 °C. The first decomposition step within the range 45–205 °C corresponds to the loss of one water molecule with mass loss of 2.16% (calcd 3.20%). The second step corresponds to a mass loss of 11.25% (calcd 12.8%) within the temperature range 205–415 °C and represents the loss of Cl_2 gas. The last three steps, 415–995 °C with a mass loss of 72.48% (calcd 69.50%), are reasonably accounted for by the decomposition of the organic part of the complex $C_{22}H_{16}O_3N_4$ leaving CuO as a residue.

The Zn(II) complex thermally decomposes in four stages. The first stage corresponds to a mass loss of 36.92% (calcd 36.56%) within the range 45–305 °C representing the loss of Cl_2 gas and $C_5H_5O_2N_2$. The second stage corresponds to a mass loss of 23.39% (calcd 22.76%) within the range 305–450 °C and represents the loss of $C_6H_6ON_2$. The third and fourth steps, 450–995 °C with a mass loss of 25.51% (calcd 25.55%), are reasonably attributed to the decomposition of the remaining organic part of the complex $C_{11}H_5$ leaving ZnO as a residue with mass percent of 14.10% (calcd 15.13%).

The TG curve of the Cd(II) complex shows four steps of decomposition. The first step occurs in the range 45–225 °C and is associated with the loss of H_2O molecule and HCl gas with an estimated mass loss of 8.37% (calcd 9.34%). The second step occurs in the range 225–425 °C and is associated with the loss of HCl gas and $C_5H_4N_2$ molecule and with an estimated mass loss of 22.15% (calcd 22.02%). The third and fourth steps are within the range 425–995 °C which are assigned to the loss of $C_{17}H_{10}O_3N_2$ with a mass loss of 50.83% (calcd 49.70%). The residue corresponds to cadmium oxide with mass percent 18.79% (calcd 18.94%).

3.11 | Biological activity

The Schiff base ligand and its mixed ligand chelates were evaluated for antimicrobial activity against Gram-positive bacteria (*Streptococcus pneumoniae* and *Bacillus subtilis*), Gram-negative bacteria (*Pseudomonas aeruginosa* and *Escherichia coli*) and fungi (*Aspergillus fumigatus* and *Candida albicans*) using the diffusion agar technique. The inhibition zone diameter was measured in millimetres and the results for the tested compounds are summarized in Table 4 and shown in Figure 4. Ampicillin, gentamicin and amphotericin were used as standard antibiotics for Gram-positive bacteria, Gram-negative bacteria and fungi, respectively. On comparing the antimicrobial activity of the Schiff base ligand and some of its transition metal complexes, the following results were obtained.

3.11.1 | *Streptococcus pneumoniae* and *Bacillus subtilis*

The biological activity of the Schiff base ligand is found to be less than that of the ampicillin standard, while Mn(II) and Cd(II) complexes are found to have activity equal to that of the standard and higher than that of ligands L^1 and L^2. It is obvious that the order of activity is as follows: Mn(II) = Cd(II) = ampicillin > Zn(II) > Cr(III) > Cu(II) > Ni(II) > L^1 > Fe(III) > Co(II) > L^2.

TABLE 4 Biological activity of L^1, L^2 and mixed ligand complexes

	Inhibition zone diameter (mm mg^{-1})					
	Fungi		Gram positive		Gram negative	
Ligand/complex	Aspergillus fumigatus	*Candida albicans*	Streptococcus pneumoniae	Bacillus subtilis	Pseudomonas aeruginosa	*Escherichia coli*
L^1	13.7	11.7	14.5	15.2	12.9	12.7
L^2	NA	NA	9.6	12.5	10.3	12.9
$[Cr(L^1)(L^2)]Cl_3$	20.6	17.6	18.3	22.6	19.3	17.8
$[Mn((L^1)(L^2)]Cl_2$	23.7	25.4	23.8	32.4	17.3	19.9
$[Fe(L^1)(L^2)]Cl_3$	18.7	10.9	12.9	13.2	11.8	10.8
$[Co(L^1)(L^2)]Cl_2$	17.6	11.3	12.3	12.7	10.1	8.5
$[Ni(L^1)(L^2)]Cl_2$	15.7	13.3	14.6	15.9	10.2	9.8
$[Cu(L^1)(L^2)]Cl_2{\cdot}H_2O$	16.2	14.1	16.9	18.2	9.8	11.9
$[Zn(L^1)(L^2)]Cl_2$	22.3	12.3	19.5	29.8	12.3	17.6
$[Cd(L^1)(L^2)]Cl_2{\cdot}H_2O$	23.7	25.4	23.8	32.4	17.3	19.9
Amphotericin	23.7	25.4	—	—	—	—
Ampicillin	—	—	23.8	32.4	—	—
Gentamicin	—	—	—	—	17.3	19.9

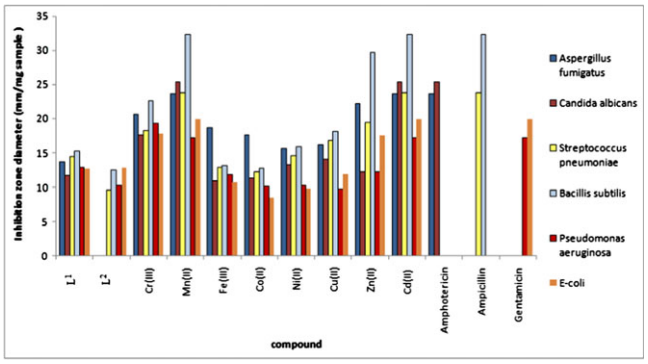

FIGURE 4 Antibacterial and antifungal activities of Schiff base ligand and its mixed ligand complexes

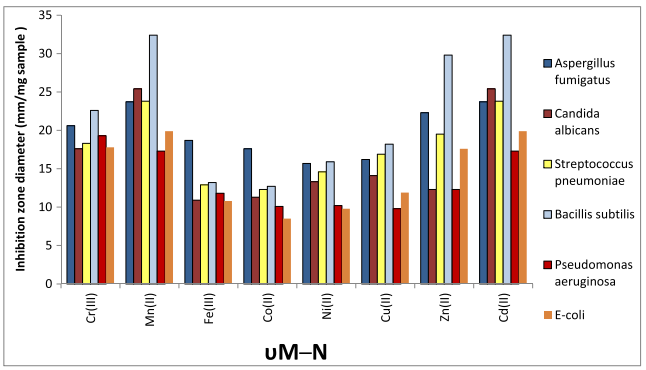

FIGURE 5 Antibacterial and antifungal activities of ν(M─N) of mixed ligand complexes

3.11.2 | *Pseudomonas aeruginosa*

The data listed in Table 4 show that the biological activity of the Cr(III) complex is higher than that of gentamicin standard and ligands L^1 and L^2. The free Schiff base ligand has lower biological activity than the standard. The order of the biological activity of the compounds is found to be: Cr(III) > gentamicin = Mn(II) = Cd(II) > L^1 > Zn(II) > Fe(III) > L^2 > Ni(II) > Co(II) > Cu(II).

3.11.3 | *Escherichia coli*

The Mn(II) and Cd(II) complexes have the same biological activity as gentamicin standard and higher biological activity than ligands L^1 and L^2. The bacterial growth inhibitory capacity of the ligands and mixed ligand complexes follows the order Mn(II) = Cd(II) = gentamicin > Cr(III) > Zn(II) > L^2 > L^1 > Cu(II) > Fe(III) > Ni(II) > Co(II).

3.11.4 | *Aspergillus fumigatus* and *Candida albicans*

It is found that the antifungal activity of the standard is higher than that of the free Schiff base ligand and equal to that of Mn(II) and Cd(II) complexes which have higher biological activity than the other complexes. It is obvious that ligand L^2 has no antifungal activity against *A. fumigatus*. The order of the antifungal activity is found to be: Mn(II) = Cd(II) = amphotericin > Zn(II) > Cr(III) > Fe(III) > Co(II) > Cu(II) > Ni(II) > L^1 > L^2 for *A. fumigatus* and Mn(II) = Cd(II) = amphotericin > Cr(III) > Cu(II) > Ni(II) > Zn(II) > L^1 > Co(II) > Fe(III) > L^2 for *C. albicans*.

The effect of nitrogen and oxygen atoms that are coordinated to metal ions against some bacteria and fungi is shown in Figures 5 and 6, respectively. It is clearly noticed that the coordination of nitrogen and oxygen atoms of the ligands to the metal ions, forming chelates, increases the biological activity of the chelates compared to the free Schiff base ligand.[60,61] It has been concluded from studies that the activity of mixed ligand complexes is higher as compared to ligands, and the presence of bulky substituents

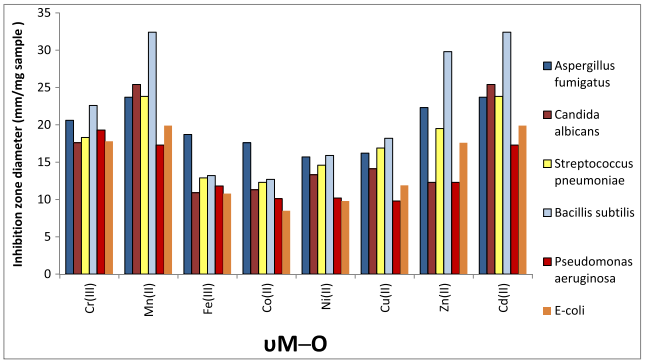

FIGURE 6 Antibacterial and antifungal activities of ν(M─O) of mixed ligand complexes

may be responsible for the enhancement of biological activity.[62–64]

Also, we could explain the enhancement in the antimicrobial activity on the basis of the ligand structure and by the presence of azomethine (C═N) group which is important in elucidating the mechanism of transamination and resamination reactions in biological systems.[65,66] It has also been suggested[67,68] that ligands with nitrogen and oxygen donor systems might inhibit enzyme production, since the enzymes that require these groups for their activity appear to be especially susceptible to deactivation by metal ions upon chelation. Chelation reduces the polarity[67–69] of a metal ion mainly because of the partial sharing of its positive charge with the donor groups and possibly π-electron delocalization within the whole chelate ring system thus formed during coordination. The chelation process increases the lipophilic nature of the central metal atom, which in turn favours its permeation through the lipoid layer of a cell membrane. In turn it is responsible for increasing the hydrophobic character and liposolubility of the molecule in crossing cell membrane of a microorganism, and hence enhances the biological utilization ratio and activity of the compounds under investigation. The results also show that the nature of the metal and the coordinated metal ion play significant roles in the inhibition activity.[70,71]

3.12 | Anticancer activity evaluation

The cytotoxicity of the new Schiff base ligand and its mixed ligand complexes with 2,2′-bipyridine against tumour cell lines (MCF-7, breast cancer; and HCT-116, colon cancer) was evaluated. The mode of anti-tumour activity can be determined using various concentrations of free Schiff base ligand, 2,2′-bipyridine ligand and mixed ligand complexes as shown in Figures 7 and 8 for MCF-7 and HCT-116, respectively. It is observed that the free Schiff base ligand, Co(II) and Cu(II) complexes are inactive with inhibition ratio less than 70%, while other complexes show much higher activity against MCF-7 cell line with the following order: Fe(III) > Cd(II) > Cr(III) > Ni(II) > Zn(II) > L^2 > Mn(II). On the other hand, Cu(II) and Cd(II) complexes are almost inactive (inhibition ratio less than 70%) while ligands and mixed ligand complexes show moderate to high activity against colon cancer cell line with the following order: Co(II) > Cr(III) > Ni(II) > L^2 > Mn(II) > Fe(III) > L^1 > Zn(II). It is clear that Co(II) complex is very active against HCT-116 colon cancer cell line compared to the other compounds with inhibition ratio higher than 90%. The IC_{50} values range from 3.99 to 41.4 and 5.81 to 35.80 μg ml^{-1} for breast cancer and colon cancer cell lines, respectively. The results are summarized in Table 5 and shown in Figure 9.

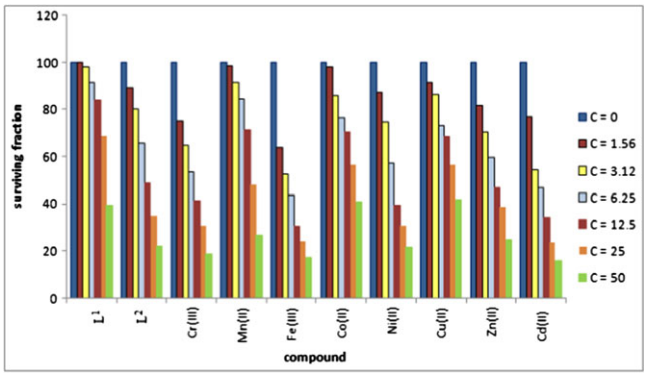

FIGURE 7 Anticancer activities of Schiff base ligand and its mixed ligand complexes for MCF-7 cell line (breast cancer)

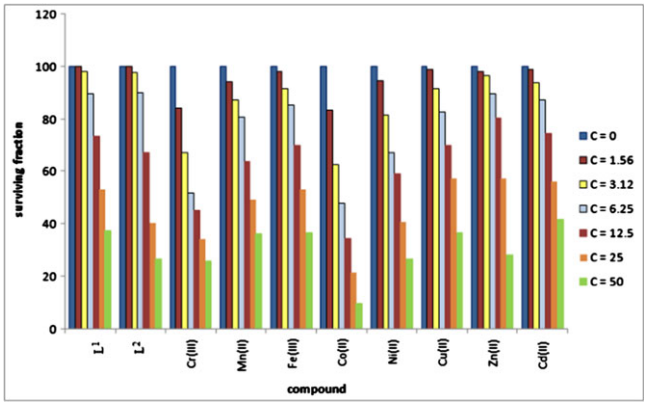

FIGURE 8 Anticancer activities of Schiff base ligand and its mixed ligand complexes for HCT-116 cell line (colon cancer)

TABLE 5 IC_{50} values for MCF-7 (breast cancer) and HCT-116 (colon cancer) cell lines of Schiff base ligand (L^1) and its mixed ligand complexes

Ligand/complex	IC_{50} (μg $μl^{-1}$)	
	MCF-7	HCT-116
L^1	41.1	29.6
L^2	12	20
$[Cr(L^1)(L^2)]Cl_3$	8.09	7.94
$[Mn((L^1)(L^2)]Cl_2$	23.8	24.2
$[Fe(L^1)(L^2)]Cl_3$	3.99	29.4
$[Co(L^1)(L^2)]Cl_2$	35.4	5.81
$[Ni(L^1)(L^2)]Cl_2$	8.8	18.6
$[Cu(L^1)(L^2)]Cl_2{\cdot}H_2O$	36	33.9
$[Zn(L^1)(L^2)]Cl_2$	11	31.2
$[Cd(L^1)(L^2)]Cl_2{\cdot}H_2O$	4.98	35.8

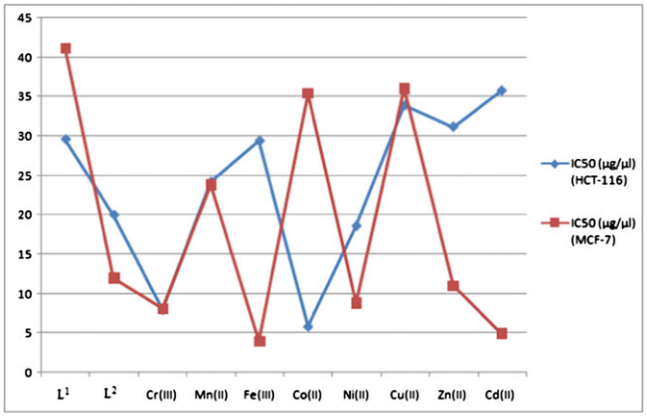

FIGURE 9 IC_{50} values for HCT-116 (colon cancer) and MCF-7 (breast cancer) cell lines of Schiff base ligand (L^1) and its mixed ligand complexes

4 | CONCLUSIONS

A new Schiff base ligand and its Cr(III), Mn(II), Fe(III), Co(II), Ni(II), Cu(II), Zn(II) and Cd(II) mixed ligand complexes were prepared and characterized using various spectral and physicochemical methods. The Schiff base ligand performed as a neutral tetradentate ligand and was coordinated to the central metal ions through the azomethine N and furan O. The IR spectral data indicated that Schiff base and 2,2′-bipyridine ligands coordinated to the metal ions by N of azomethine and pyridine, respectively, and furan O. The molar conductance showed that all complexes are electrolytes. The solid reflectance spectra of all complexes and the ESR spectrum of the Cu(II) complex were used to confirm their octahedral geometry. The thermal decomposition of the complexes was used to support the suggested molecular formulae and to determine the stability of the Schiff base and 2,2′-bipyridine ligands and the mixed ligand chelates. The biological activities of L^1 and L^2 and the mixed ligand chelates were tested against various fungal and bacterial organisms. The results showed that the Mn(II) and Cd(II) complexes mostly had higher biological activity than the

Schiff base ligand and other chelates. It was also observed that the free Schiff base ligand and Co(II) and Cu(II) complexes were inactive against breast cancer cell line (MCF-7) while other complexes showed much higher activity against the same cell line. On the other hand, the Co(II) complex was very active against colon cancer cell line (HCT-116) compared to the other compounds, and the Schiff base ligand and Cd(II) complex were almost inactive.

REFERENCES

[1] S. A. Hosseini-Yazdi, P. Samadzadeh-Aghdam, A. Mirzaahmadi, A. A. Khandar, G. Mahmoudi, M. Ruck, T. Doert, S. S. Balula, L. Cunha-Silva, *Polyhedron* **2014**, *80*, 41.

[2] J. Anacona, J. Santaella, *Spectrochim. Acta A* **2013**, *115*, 800.

[3] A. D. Garnovskii, A. L. Nivorozhkin, V. I. Minkin, *Coord. Chem. Rev.* **1993**, *126*, 1.

[4] R. Ziessel, *Coord. Chem. Rev.* **2001**, *216*, 195.

[5] E. Yousif, A. Majeed, K. Al-Sammarrae, N. Salih, J. Salimon, B. Abdullah, *Arab. J. Chem.* **2013**, DOI: 10.1016/j.arabjc.2013.06.006

[6] S. Annapoorani, C. N. Krishnan, *Int. J. Chem. Technol. Res.* **2013**, *5*, 180.

[7] S. M. Devidas, S. H. Quadri, S. A. Kamble, F. M. Syed, D. Y. Vyavhare, *J. Chem. Pharm. Res.* **2011**, *3*, 489.

[8] A. J. Xavier, M. A. Raj, J. M. Marie, *J. Chem. Pharm. Res.* **2012**, *4*, 669.

[9] M. Padmaja, J. Pragathi, C. G. Kumari, *J. Chem. Pharm. Res.* **2011**, *3*, 602.

[10] B. R. Thorat, R. Jadhav, M. Mustapha, S. Lele, D. Khandekar, P. Kamat, S. Sawant, D. Arakh, R. G. Atram, R. Yamgar, *J. Chem. Pharm. Res.* **2011**, *3*, 1045.

[11] N. Raman, R. Y. Pitchaikani, A. Kulandaisamy, *Proc. Indian Acad. Sci. (Chem. Sci.)* **2001**, *113*, 183.

[12] A. P. Mishra, *K. Rajendra. J. Chem. Pharm. Res.* **2010**, *2*, 51.

[13] H. C. Freeman, in *Inorganic Biochemistry*, (Ed: G. L. Eichhorn) Vol. 1, Elsevier, Amsterdam **1973**, 121.

[14] R. P. Ajay, J. D. Kamini, S. R. Sambhaji, R. P. Vishwanath, S. L. Rama, *J. Chem. Pharm. Res.* **2012**, *4*, 1413.

[15] G. G. Mohamed, M. M. Omar, A. M. Hindy, *Turk. J. Chem.* **2006**, *30*, 361.

[16] R. D. Jones, D. A. Summerville, F. Basolo, *Chem. Rev.* **1979**, *79*, 139.

[17] G. H. Olie, S. Olive, *The Chemistry of the Catalyzes Hydrogenation of Carbon Monoxide*, Springer, Berlin **1984**.

[18] J. D. Margerum, L. J. Miller, in *Photochromism*, (Ed: G. H. Brown), Wiley-Interscience, New York **1971**, 569.

[19] W. J. Sawodny, M. Riederer, *Angew, Chem. Int. Ed. Engl.* **1977**, *16*, 859.

[20] W. H. Mahmoud, N. F. Mahmoud, G. G. Mohamed, A. Z. El-Sonbati, A. A. El-Bindary, *J. Mol. Struct.* **2015**, *1095*, 15.

[21] A. T. Chaviara, P. J. Cox, K. H. Repana, R. M. Papi, K. T. Papazisis, D. Zambouli, A. H. Kortsaris, D. A. Kyriakidis, C. A. Bolos, *J. Inorg. Biochem.* **2004**, *98*, 1271.

[22] J. A. Ciller, C. Seoane, J. L. Soto, B. Yruretagoyena, *J. Heterocycl. Chem.* **1986**, *23*, 1583.

[23] O. A. M. Ali, *Spectrochim. Acta A* **2014**, *132*, 52.

[24] R. J. Harrison, M. Moyle, *Org. Synth. Coll.* **1963**, *4*, 493.

[25] A. Dobosz, J. Spychała, H. Kozłowski, M. Rowińska, A. Temeriusz, H. Frauendorf, F. Meyer, *J. Inorg. Biochem.* **2007**, *101*, 1505.

[26] X. Luo, C. Li, Y. Liang, *Chem. Commun.* **2000**, *2091*.

[27] C. Kaes, A. Katz, M. W. Hosseini, *Chem. Rev.* **2000**, *100*, 3553.

[28] F. Blau, *Monatsh. Chem.* **1889**, *10*, 375.

[29] A. I. Vogel, *Quantitative Inorganic Analysis Including Elemental Instrumental Analysis*, 2nd ed., Longmans, London **1962**.

[30] A. C. Scott, in *Practical Medical Microbiology*, 13th ed. (Eds: J. G. Collee, J. P. Duguid, A. G. Fraser, B. P. Marmion), Churchill Livingstone, Edinburgh **1989**, 161.

[31] T. R. Mosmann, *J. Immunol. Methods* **1983**, *65*, 55.

[32] M. Hossain, S. K. Chattopadhyay, S. Ghosh, *Polyhedron* **1997**, *16*, 1793.

[33] G. G. Mohamed, M. M. Omar, A. A. Ibrahim, *Eur. J. Med. Chem.* **2009**, *44*, 4801.

[34] H. A. El-Boraey, O. A. El-Gammal, *Spectrochim. Acta A* **2015**, *138*, 553.

[35] H. F. Abd El-halim, M. M. Omar, G. G. Mohamed, *Spectrochim. Acta A* **2011**, *78*, 36.

[36] G. G. Mohamed, E. M. Zayed, A. M. M. Hindy, *Spectrochim. Acta A* **2015**, *145*, 76.

[37] O. A. M. Ali, *Spectrochim. Acta A* **2014**, 121,188.

[38] W. H. Mahmoud, G. G. Mohamed, M. M. I. El-Dessouky, *J. Mol. Struct.* **2015**, *1082*, 12.

[39] S. Ilhan, H. Baykara, A. Oztomsuk, V. Okumus, A. Levent, M. S. Seyitoglu, S. Ozdemir, *Spectrochim. Acta A* **2014**, *118*, 632.

[40] W. H. Mahmoud, R. G. Deghadi, G. G. Mohamed, *Appl. Organometal. Chem.* **2016**, *30*, 221.

[41] G. G. Mohamed, N. E. A. El-Gamel, *Spectrochim. Acta A* **2004**, *60*, 3141.

[42] F. A. Cotton, G. Wilkinson, C. A. Murillo, M. Bochmann, *Advanced Inorganic Chemistry*, 6th ed., Wiley, New York **1999**.

[43] H. F. Abd El-Halim, G. G. Mohamed, M. M. I. El-Dessouky, W. H. Mahmoud, *Spectrochim. Acta A* **2011**, *82*, 8.

[44] A. M. A. Alaghaz, H. A. Bayoumi, Y. A. Ammar, S. A. Aldhlmani, *J. Mol. Struct.* **2013**, *1035*, 383.

[45] C. G. Richthofen, A. Stammler, H. Bogge, T. Glaser, *Eur. J. Inorg. Chem.* **2012**, *36*, 5934.

[46] G. G. Mohamed, M. H. Solimanb, *Spectrochim. Acta A* **2010**, *76*, 341.

[47] A. M. A. Alaghaz, R. A. Ammar, *Eur. J. Med. Chem.* **2010**, *45*, 1314.

[48] B. N. Figgis, *Intoduction to Ligand Fields*, 2nd ed., Wiley, London **1966**.

[49] S. Chandra, K. Gupta, *Transit. Met. Chem.* **2002**, *27*, 196.

[50] A. Z. El-Sonbati, M. A. Diab, A. A. El-Bindary, G. G. Mohamed, S. M. Morgan, *Inorg. Chim. Acta* **2015**, *430*, 96.

[51] N. A. El-Ghamaz, A. Z. El-Sonbati, M. A. Diab, A. A. El-Bindary, G. G. Mohamed, S. M. Morgan, *Spectrochim. Acta A* **2015**, *147*, 200.

[52] M. H. Soliman, A. M. M. Hindy, G. G. Mohamed, *J. Therm. Anal. Calorim.* **2014**, *115*, 987.

[53] A. M. F. Benial, V. Ramakrishnan, R. Murugesan, *Spectrochim. Acta A* **2000**, *56*, 2775.

[54] D. Kivelson, R. Neiman, *J. Chem. Phys.* **1961**, *35*, 149.

[55] M. F. R. Fouda, M. M. Abd-el-zaher, M. M. E. Shadofa, F. A. El Saied, M. I. Ayad, A. S. El Tabl, *Transit. Met. Chem.* **2008**, *33*, 219.

[56] A. Z. El-Sonbati, M. A. Diab, A. A. El-Bindary, G. G. Mohamed, S. M. Morgan, *Inorg. Chim. Acta* **2015**, *430*, 96.

[57] N. A. El-Ghamaz, A. Z. El-Sonbati, M. A. Diab, A. A. El-Bindary, G. G. Mohamed, S. M. Morgan, *Spectrochim. Acta A* **2015**, *147*, 200.

[58] S. Velumania, X. Mathew, P. J. Sebastian, S. K. Narayandass, D. Mangalaraj, *Solar Energy Mater. Solar Cells* **2003**, *76*, 347.

[59] S. Basavaraja, D. S. Balaji, M. D. Bedre, D. Raghunandan, P. M. P. Swamy, A. Venkatarman, *Bull. Mater. Sci.* **2011**, *34*, 1313.

[60] B. G. Tweedy, *Phytopathology* **1964**, *55*, 910.

[61] S. K. Sengupta, O. P. Pandey, B. K. Srivastava, V. K. Sharma, *Transit. Met. Chem.* **1998**, *23*, 349.

[62] A. R. Patil, K. J. Donde, S. S. Raut, V. R. Patil, R. S. Lokhande, *J. Pharm. Res.* **2011**, *4*, 2256.

[63] V. K. Patel, A. M. Vasanwala, C. N. Jejurkar, *Indian J. Chem.* **1989**, *28A*, 719.

[64] Z. H. Chohan, M. Praveen, A. Ghaffar, *Metal-Based Drugs* **1997**, *4*, 267.

[65] K. Y. Lau, A. Mayr, K. K. Cheung, *Inorg. Chim. Acta* **1999**, *285*, 223.

[66] P. P. Dholakiya, M. N. Patel, *Synth. React. Inorg. Met.-Org. Chem.* **2004**, *34*, 553.

[67] Z. H. Chohan, *Synth. React. Inorg. Met.-Org. Chem.* **2004**, *34*, 833.

[68] Z. H. Chohan, C. T. Supuran, A. Scozzafava, *J. Enzyme Inhib. Med. Chem.* **2004**, *19*, 79.

[69] Z. H. Chohan, M. Arif, M. A. Akhtar, C. T. Supuran, *Bioinorg. Chem. Appl.* **2006**, *2006*, 831.

[70] A. M. Balan, R. F. Ashok, M. Vasanthi, R. Prabu, A. Paulraj, *Int. J. Life Sci. Pharma Rev.* **2013**, *3*, 67.

[71] W. Al Zoubi, A. A. Al-Hamdani, M. Kaseem, *Appl. Organometal. Chem.* **2016**, *30*, 810.

How to cite this article: Omar MM, Abd El-Halim HF, Khalil EAM. Synthesis, characterization, and biological and anticancer studies of mixed ligand complexes with Schiff base and 2,2′-bipyridine. *Appl Organometal Chem*. 2017;e3724. https://doi.org/10.1002/aoc.3724